HHS Public Access

Author manuscript

J Mol Biol. Author manuscript; available in PMC 2023 October 23.

Published in final edited form as:

J Mol Biol. 2023 June 01; 435(11): 168026. doi:10.1016/j.jmb.2023.168026.

The E3 ubiquitin ligase, CHIP/STUB1, inhibits aggregation of phosphorylated proteoforms of microtubule-associated protein tau (MAPT)

Cory M. Nadel[†,1,3], **Aye C. Thwin**[†,2,3], **Matthew Callahan**[1,3], **Kanghyun Lee**[2,3], **Emily Connelly**[1], **Charles S. Craik**[1], **Daniel R. Southworth**[*,2,3], **Jason E. Gestwicki**[*,1,3]

[1]Department of Pharmaceutical Chemistry, University of California San Francisco, San Francisco, CA 94508

[2]Department of Biochemistry & Biophysics, University of California San Francisco, San Francisco, CA 94508

[3]Institute for Neurodegenerative Diseases, University of California San Francisco, San Francisco, CA 94508

Abstract

Hyper-phosphorylated tau accumulates as insoluble fibrils in Alzheimer's disease (AD) and related dementias. The strong correlation between phosphorylated tau and disease has led to an interest in understanding how cellular factors discriminate it from normal tau. Here, we screen a panel of chaperones containing tetratricopeptide repeat (TPR) domains to identify those that might selectively interact with phosphorylated tau. We find that the E3 ubiquitin ligase, CHIP/*STUB1*, binds 10-fold more strongly to phosphorylated tau than unmodified tau. The presence of even sub-stoichiometric concentrations of CHIP strongly suppresses aggregation and seeding of phosphorylated tau. We also find that CHIP promotes rapid ubiquitination of phosphorylated tau, but not unmodified tau, *in vitro*. Binding to phosphorylated tau requires CHIP's TPR domain, but the binding mode is partially distinct from the canonical one. In cells, CHIP restricts seeding by phosphorylated tau, suggesting that it could be an important barrier in cell-to-cell spreading. Together, these findings show that CHIP recognizes a phosphorylation-dependent degron on tau, establishing a pathway for regulating the solubility and turnover of this pathological proteoform.

[*]To whom correspondence can be addressed: Jason E. Gestwicki, Sandler Neuroscience Center, 675 Nelson Rising Lane, Rm 311, San Francisco, CA 94508, (p) 415 502 7121, jason.gestwicki@ucsf.edu, Daniel R. Southworth, Sandler Neuroscience Center, 675 Nelson Rising Lane, Rm 311B, San Francisco, CA 94508, daniel.southworth@ucsf.edu.

[†]These authors contributed equally

AUTHOR CONTRIBUTIONS

C.M.N. Conceptualization, Investigation, Formal Analysis, Visualization, Writing
A.C.T. Conceptualization, Investigation, Formal Analysis, Visualization, Writing
M.C. Resources
K.L. Resources
E.C. Resources
C.S.C Supervision, Resources
D.R.S Conceptualization, Formal Analysis, Supervision, Writing
J.E.G. Conceptualization, Formal Analysis, Supervision, Writing

DISCLOSURES

J.E.G. is a co-founder of Kaizen Therapeutics and a consultant for Protego and DiCE. The other authors have no conflicts to disclose.

Keywords

protein-protein interactions; protein aggregation; tauopathy; intrinsically disordered protein; phospho-degrons; ubiquitination; C-terminus of Hsp70-interacting protein

INTRODUCTION

Accumulation of microtubule-associated protein tau (*MAPT*/tau) in neurofibrillary tangles (NFTs) underlies a class of fatal and incurable neurodegenerative diseases referred to as tauopathies [1]. Tau is a soluble, intrinsically disordered protein that normally functions to stabilize tubulin dimers and regulate cytoskeletal dynamics [2–4]. During the pathogenesis of tauopathies, tau becomes hyperphosphorylated, resulting in a weakened affinity for microtubules [5], a greater tendency to aggregate [6] and, in some cases, an enhanced ability to act as a seed in cell-to-cell spreading assays [7, 8]. Hyperphosphorylated tau has also been observed in brain tissues from tauopathy patients, where it corelates with disease severity [9–12]. Based on these observations, phosphorylated tau has long been considered to be a pathological proteoform and; therefore, it is important to understand the factors that maintain its protein homeostasis (proteostasis).

Proteostasis is the balance of protein synthesis, folding and turnover and it is normally maintained by a collection of chaperones and quality control pathways, collectively termed the proteostasis network. Many components of the proteostasis network are known to bind to tau and regulate its levels. For example, members of the heat shock protein 70 (Hsp70) family of molecular chaperones bind directly to tau after its release from microtubules [13], limiting tau aggregation and promoting its turnover under some conditions [14, 15]. Chemically stabilizing the Hsp70-tau interaction enhances tau turnover [16, 17], showing the importance of this pathway as a putative drug target. Within the broader proteostasis network, Hsp70s collaborate with a series of co-chaperones [18]. Recent evidence suggests that several of these co-chaperones can also modulate tau aggregation and that some of them operate independent of Hsp70s [19–21]. For example, the co-chaperone, DnaJC7, was recently shown to suppress tau aggregation *in vitro* and limit formation of tau seeds [22]. While this is an exciting result, it was found that DnaJC7 was less effective against phosphorylated tau. Indeed, in a screen of ~30 chaperones and co-chaperones, most of them, except Hsp27 [23], had significantly weaker binding to pseudo-phosphorylated tau [19]. These findings suggest that relatively few components of the proteostasis network might recognize phosphorylated tau proteoforms.

DnaJC7 belongs to a family of TPR-containing co-chaperones, which includes the protein phosphatase 5 (*PPP5C*/PP5) and C-terminus of Hsp70-interacting protein (*STUB1*/CHIP). Interestingly, many of the TPR proteins have been linked to tau proteostasis and some, including DnaJC7, have been found to bind directly to tau [24–28]. These results suggest that the TPR domain might be well suited to binding tau. However, it is not yet clear whether any of the TPR proteins might bind phosphorylated tau. Here, we purify both unmodified tau and phosphorylated tau (p.tau), and then test a panel of TPR co-chaperones for their ability to suppress aggregation using thioflavin T (ThT) and electron microscopy (EM). We

find that a subset of TPR proteins have anti-aggregation activity, but that CHIP is the most potent at inhibiting p.tau aggregation, even retaining activity against a disease-associated mutation, P301S. CHIP is an E3 ubiquitin ligase and we find that it rapidly ubiquitinates p.tau, but not tau, *in vitro*, suggesting that the binding site creates a phospho-degron. Finally, we show that CHIP restricts p.tau seeding in cells, in a mechanism that require both its ubiquitin ligase activity and its collaboration with Hsp70s. Together, these studies suggest that phosphorylation of tau creates a binding site for CHIP, providing a potential mechanism for cells to counteract the accumulation, aggregation and spreading of phosphorylated tau proteoforms.

RESULTS

Amongst the TPR chaperones, CHIP preferentially suppresses p.tau aggregation

To identify TPR co-chaperones that might suppress phosphorylated tau aggregation, we first performed thioflavin T (ThT) assays using the panel of TPR proteins: DnaJC7, HOP, PP5, and CHIP. In these experiments, we utilized recombinant tau proteins purified from either *E. coli*, to produce tau devoid of post-translational modifications (PTMs), or Sf9 insect cells, to produce phosphorylated tau (p.tau) [29]. By mass spectrometry, the p.tau produced in this way is phosphorylated at 21 sites, including those sites commonly observed in pathological tau (Fig S1A, S1B). We also confirmed a subset of these pathological modifications, including pT231, by immunoblot using phospho-specific antibodies (Fig S1C).

In the ThT assays, we defined anti-aggregation activity of TPR proteins based on their ability to delay the onset of tau or p.tau aggregation, termed the “lag time”. Consistent with previous findings [22], DnaJC7 increases the lag time by approximately 4-fold (Fig 1A,B), while it is significantly less active against p.tau (Fig 1C, D). The TPR proteins, HOP and PP5, have minimal effect on either tau or p.tau, showing that anti-aggregation activity is not a shared property of all TPR domains. Finally, we find that CHIP extends the lag time of unmodified tau by a modest ~2-fold, but that it has an especially dramatic effect on p.tau aggregation, extending lag time by 5-fold (Fig 1C, D). Thus, of the TPR proteins screened here, CHIP seems to be the most potent at delaying p.tau aggregation and it is partially selective for this proteoform.

While ThT fluorescence is a useful surrogate for amyloid formation, we also characterized the aggregation reactions using negative stain electron microscopy (EM). We studied the samples at 48 hrs, which is long after the TPR protein-mediated lag-time extension, to understand whether the tau eventually forms characteristic amyloids (*e.g.*, twisted and straight fibrils with a diameter of ~25–30 nm and insoluble by centrifugation [30]). For the unmodified tau samples, we indeed observe fibrils of the expected morphologies by EM, regardless of which TPR co-chaperone is added (Fig 1E). However, a different result is obtained with the samples containing p.tau. Although HOP- and PP5-treated samples contain characteristic amyloids by EM, addition of CHIP or DnaJC7 instead results in protofibrils and poorly formed aggregates (Fig 1E). Taken together, these results support the conclusion that a subset of TPR proteins maintain the solubility of p.tau and suppress the

formation of amyloid fibrils. Of these active proteins, CHIP appears to have a particularly strong effect on the p.tau proteoforms.

CHIP preferentially inhibits aggregation and seeding of phosphorylated tau

To better characterize the binding of CHIP to p.tau, the strength of the interaction was measured by ELISA. Strikingly, we find that CHIP binds p.tau ~10-fold (K_d = 0.44 ± 0.02 μM) better than it binds to unmodified tau (K_d = 6.25 ± 0.24 μM) (Fig 2A, B). Because CHIP is an E3 ubiquitin ligase, we wondered whether this binding might result in ubiquitination. Indeed, in the presence of a reaction mixture *in vitro*, CHIP strongly ubiquitinates p.tau, but not tau (Fig 2C). Even at short incubation times (1 min), most of the p.tau is modified with large ubiquitin chains, as evident by conversion of the monomer to a series of high molecular mass bands. We then used mass spectrometry to map the location(s) of these ubiquitin modifications, revealing that p.tau is ubiquitinated at multiple sites, including those that are not found on the non-phosphorylated tau samples (Fig S2). Given its strong affinity, we hypothesize that CHIP might suppress p.tau aggregation at relatively low concentrations. Indeed, in dose dependence ThT studies, an equimolar amount of CHIP is required to suppress aggregation of unmodified tau (Fig 2D, 2E) but it is active at substoichiometric ratios for p.tau, even suppressing aggregation at 1/5th the p.tau concentration (Fig 2F, 2G).

Finally, we queried whether CHIP could suppress the formation of tau and p.tau seeds, using a biosensor cell line [31, 32]. These experiments are of particular interest given that we observed some aggregates in the CHIP-treated p.tau samples by EM (see Fig 1C), which we thought might retain seeding activity. In the seeding experiments, we used a previously established protocol wherein tau seeds are generated *in vitro*, complexed with a lipid carrier Lipofectamine 2000 (L2K), and then delivered to HEK293T biosensor cells (Fig 2H). These cells constitutively express a copy of the tau repeat domain (tauRD; see Methods) bearing two pathogenic mutations (P301L, V337M) and fused to mClover. Following an incubation period with the seeds, the tauRD reporter forms punctate structures that can be readily identified (Fig 2I) and quantified (Fig 2J) using automated, high content microscopy. In control experiments, we observe negligible puncta formation (~5% cells with aggregates) following 72-hour incubation with Lipofectamine alone or Lipofectamine plus CHIP, establishing a low baseline signal. Then, to test for seeds in the CHIP-treated tau and p.tau samples, we pre-formed them for 24 hours, as described above, and then used the samples to treat the biosensor cells. The results show that CHIP is unable to significantly suppress the seeding of unmodified tau (~25% of cells with aggregates), but that it largely abrogates the formation of p.tau seeds (~5% of cells with aggregates; Fig 2I, J). Together, these studies show that CHIP suppresses p.tau aggregation at sub-stoichiometric concentrations *in vitro* and that it prevents the formation of p.tau seeds.

CHIP restricts aggregation and seeding of disease-associated P301S mutant phospho-tau

Several genetic mutations in the *MAPT* gene are associated with tauopathies [33]. The P301S mutation is of particular interest because it is closely associated with some forms of frontotemporal dementia (FTD) and the P301S protein has been found to be more aggregation-prone than wildtype [34]. Importantly, many *MAPT*/tau mutations are known

to weaken interactions with proteostasis components, such as Hsp70 and DnaJC7 [19, 22]. Indeed, this ability to partially "avoid" the proteostasis network is thought to contribute to their accumulation. To probe whether P301S p.tau might likewise limit binding to TPR proteins, we purified P301S p.tau proteins from Sf9 cells and screened these against DnaJC7, HOP, PP5 and CHIP via ThT assays. Consistent with WT p.tau, we find that CHIP also retains the ability to significantly extend the lag time of the P301S p.tau (Fig 3A, 3B). Consistent with this conclusion, we find that CHIP binds equally well to both wild type and P301S p.tau (Fig 3C, 3D), using ELISAs. To test the relative potency of CHIP for P301S p.tau, we repeated the ThT assays using a range of CHIP concentrations. We observe that equimolar concentrations of CHIP, rather than sub-stoichiometric levels, are required (Fig 3E), perhaps because P301S p.tau is significantly more aggregation prone than WT p.tau. Finally, we tested whether CHIP suppresses the formation of P301S p.tau seeds, using the HEK293T biosensor cells. While CHIP completely abrogates seeding by WT p.tau, it has slightly reduced activity against P301S p.tau (Fig 3F). Thus, these results show that CHIP largely retains activity against the FTD-associated, P301S mutant tau.

CHIP recognizes p.tau through a distinct TPR binding mode

Previous studies have shown that DnaJC7's TPR domain is required for binding to tau [22], so we hypothesized that equivalent interactions might also be required for CHIP binding to p.tau. The TPR domain of CHIP is known to bind with tight affinity (Kd ~ 0.62 μM) to a fluorescence polarization (FP) tracer corresponding to the last 10 amino acids of Hsc70/*HSPA8* (Fig 4A) [35]. Thus, we pre-incubated this tracer with full-length CHIP and then titrated with tau or p.tau to determine if these proteins bind in the canonical TPR cleft. Consistent with previous studies [36], our FP experiments show that unmodified tau binds weakly to the TPR domain (Ki > 10 μM). However, p.tau competes with a significantly tighter apparent affinity (Ki ~ 3 μM; Fig 4B). This result suggests that p.tau indeed binds in the canonical binding mode. To test this idea, we mutated one of the key carboxylate clamp residues, creating a K30A CHIP variant that is known to have weak affinity for the Hsc70 peptide tracer [35]. We hypothesized that K30A CHIP might have weaker affinity for p.tau and, therefore, would be less active against p.tau in ThT assays. However, we instead find that K30A CHIP suppresses aggregation of p.tau similar to WT CHIP (Fig 4C). While we were unable to accurately determine lag times under these conditions, we did observe a significant suppression of max p.tau ThT fluorescence by both WT and mutant CHIP, but no respective suppression of max ThT fluorescence for unmodified tau (Fig 4D). Together, these results suggest that CHIP's TPR domain is involved in binding p.tau, but that the interaction mode is somewhat distinct from the canonical one.

These findings suggest that p.tau contains at least one phospho-degron that binds directly to CHIP's TPR domain. In an attempt to identify the location of these phosphosites, we cross-referenced our mass spectrometry-based phospho-data (see Fig S1) against a bioinformatic tool for predicting peptides that bind to CHIP's TPR domain, called CHIPScore [26]. Briefly, CHIPScore uses a biophysics-based dataset to predict the affinity of 5-mer peptide sequences with high accuracy ($R^2 = 0.86$). Scanning the phospho-peptide data, we find only one predicted CHIP-binding ligand in p.tau, centered on pS214 and pT212 (Fig S3A). We subsequently synthesized the acetylated 10-mer peptide corresponding to this region of

tau (amino acids 208–217), containing either single or double phosphorylations and tested binding of these peptides to CHIP using FP and differential scanning fluorimetry (DSF). None of the peptides liberate the Hsc70 fluorescent tracer from CHIP (Fig S3B), nor do they significantly stabilize CHIP's thermal stability by DSF (Fig S3C, S3D). Thus, this peptide region in p.tau does not seem to be sufficient to act as the CHIP-binding site. Because the interaction of p.tau with CHIP's TPR domain is not entirely canonical, it seems possible that CHIPScore might not be the right tool to predict the binding site. In addition, an alternative interpretation is that the ability of phosphorylation to enhance CHIP binding might be mediated by changes in p.tau's conformation.

The CHIP TPR domain is required for anti-aggregation activity

Although p.tau does not rely on the K30 clamp residue, it still displaces a fluorescent Hsc70 tracer from CHIP in FP assays (see Fig 4B), suggesting that parts of the canonical binding mode might still be important. To test this idea, we utilized CHIPOpt, a high affinity (K_d ~ 0.016 μM) orthosteric inhibitor of CHIP's TPR domain. Briefly, CHIPOpt makes multiple polar and hydrophobic contacts with the TPR domain, including in the carboxylate clamp (K30 and K95), the hydrophobic shelf and nearby residues [26] (Fig 5A). Using this chemical tool, we first tested whether the TPR domain contact was required for CHIP-dependent ubiquitination of p.tau *in vitro*. Indeed, we found that addition of CHIPOpt decreases p.tau ubiquitination, with little effect on unmodified tau (Fig 5B). We then tested whether CHIPOpt would also inhibit the ability of CHIP to slow p.tau aggregation using ThT assays. Consistent with the hypothesis, CHIPOpt completely restores aggregation of tau (Fig 5C, 5D), p.tau (Fig 5E, 5F) and P301S p.tau (Fig 5G, 5H). Stoichiometric levels of CHIPOpt are needed to restore activity on tau, while an excess (5x, 20x) is needed for p.tau and P301S p.tau, consistent with the relative affinity constants from ELISA. Based on these results, we conclude that the canonical, hydrophobic cleft in the TPR domain is required for CHIP's observed anti-aggregation activity.

Endogenous CHIP restricts seeded aggregation of phospho-tau

To this point, we had studied CHIP's activity on p.tau *in vitro*. Next, we pivoted to testing its roles in cells, returning to the HEK293T biosensor cells that expresses the tagged, tau repeat domain (tauRD). Using CRISPR-Cas9, we generated a variant of this biosensor line in which CHIP/*STUB1* is deleted (*CHIP KO*). In these cells, we then stably re-introduced WT CHIP or mutant versions of CHIP that do not interact with Hsp70 (K30A) or that lack ubiquitin ligase activity (H260Q). In these cells, we first tested whether CHIP and its variants would bind to tauRD using co-immunoprecipitation. As expected, we find that re-introduction of WT CHIP or H260Q CHIP allows co-immunoprecipitation of a stable complex of CHIP and the tauRD (Fig 6A). This complex also included significant amounts of Hsp70. Interestingly, when we compared the amount of bound Hsp70 in the parent HEK293T cells to the CHIP KO, we find that less Hsp70 was pulled down with tauRD in the absence of CHIP. This result suggests that CHIP might be necessary to form a stable complex between Hsp70 and tauRD under these conditions. Consistent with the idea of a ternary complex, we observe only a modest interaction of CHIP K30A with tauRD and a significant reduction in bound Hsp70. Because the K30A mutation has little effect on the interaction of p.tau with CHIP (see Fig 4C), we conclude that weakening the Hsp70

interaction, via mutating the carboxylate clamp, might destabilize the entire complex in cells.

Next, we tested CHIP's role in restricting seeding activity in the HEK293T cells. As performed above (see Fig 2H, 3F), fibrils formed from unmodified tau or p.tau were introduced to the cells with Lipofectamine and the levels of seeding measured by high content microscopy. We find that the presence of CHIP or its variants has little effect on seeding by fibrils formed from unmodified tau (Fig 6B). In contrast, when challenged with p.tau seeds, the CHIP KO cells produce a greater number of cells with aggregates (Fig 6B). This increased seeding is rescued by reintroduction of WT CHIP, but not the K30A or H260Q mutants. Together, these results suggest that CHIP inhibits seeding of p.tau through both its interactions with Hsp70 and its ubiquitin-ligase activity (Fig 6C). Thus, CHIP seems to restrict seeding by p.tau proteoforms, which might be an important function in limiting p.tau spreading.

Discussion

Previous studies have suggested that CHIP is one of tau's physiologically relevant ubiquitin ligases [37–39]. For example, the $CHIP^{-/-}$ mouse accumulates multiple tau species in the brain, including phosphorylated tau [37], and, conversely, tau levels are reduced in a transgenic CHIP over-expression model [40]. Moreover, in AD patient brains, CHIP protein levels are reduced, concomitant with the accumulation of toxic tau proteoforms [26, 41]. Together, these observations have inspired studies aimed at understanding how CHIP binds to tau. One of the emerging themes from that work is that CHIP binds different tau proteoforms in a variety of distinct ways. For example, recent work has shown that CHIP binds directly to specific sites on unmodified tau [36], without the need for Hsp70s. However, early studies showed that CHIP seems to prefer phosphorylated tau in cells and that Hsp70s are somehow involved in forming this complex [38], suggesting that other mechanisms must also be involved. One alternative is that CHIP binds directly to a truncated proteoform of tau, tauC3 [42], which is produced by caspase cleavage [26]. Indeed, the $CHIP^{-/-}$ mouse accumulates the tauC3 proteoform [37], suggesting that this is a relevant mechanism *in vivo*. However, that mechanism does not account for CHIP's apparent activity on other tau proteoforms. In the current report, we show that CHIP binds directly to p.tau (see Fig 6C; left). This interaction suppresses p.tau's aggregation and limits formation of seeds. Like the other binding mechanisms, this interaction requires CHIP's TPR domain, although the mode seems to be distinct because the carboxylate clamp is not required. Importantly, we find that CHIP binding to p.tau rapidly generates polyubiquitin chains, suggesting that the binding site(s) act as a phospho-degron. There is precedent for this type of mechanism, because CHIP has been found to mediate turnover of other clients, such as CYP3A4, by binding phosphorylation-dependent degrons [43, 44]. *In vitro*, we find that CHIP is able to bind p.tau in the absence of Hsp70s. However, in cells, we report that CHIP selectively restricts p.tau seeding (see Fig 6C; right) and that this activity involves both collaboration with Hsp70s and the ubiquitination activity of CHIP, as judged from the fact that neither K30A nor H260Q CHIP are able to restrict p.tau seeding. Put together, we propose that the phospho-degron mechanism adds to the ways that CHIP can act on tau proteoforms. We further propose that CHIP might first recognize phospho-sites on p.tau,

after which it recruits Hsp70s, perhaps by leveraging CHIP's tendency to form dimers and oligomers. In that model, a portion of the TPR domains in a CHIP oligomer might engage p.tau, while the others would be free to bind Hsp70s. Future work is needed to understand the conditions that specifically require this phospho-degron clearance mechanism and why it fails in disease.

The proteostasis network includes ~200 proteins that are tasked with maintaining the delicate balance of protein production, folding, quality control, trafficking and turnover [18, 45]. The proteins that interact with this network are normally termed "clients" and it has become clear that some proteostasis factors are especially important for specific clients. For example, Hsp47 is critical to collagen folding [46], but less important for other clients. One of the broader implications of our current work is that each proteoform of tau (*e.g.*, truncated, phosphorylated, acetylated, splice isoform, *etc.*) might potentially be considered as a distinct client – potentially requiring different parts of the proteostasis network. More broadly, a growing number of studies are revealing that the diversity of proteoforms far surpasses the number of protein-coding genes in the human genome [47]. Thus, it seems logical that components of the proteostasis network might distinguish between proteoforms, rather than just proteins. For example, in the case of tau, it seems that unmodified tau is a relatively good client for Hsp70 and DnaJC7 [22], while p.tau is the preferred client for CHIP and Hsp27 [23]. Another interesting example of this proteoform selectivity is found in the chaperone, clusterin, which stabilizes oligomeric tau and enhances its seeding properties [20]. Based on these findings and others, we suggest that each proteoform of tau might be best considered as a separate client, and that it will be important to identify the proteostasis factors that are selective for each.

MATERIALS AND METHODS

Cell culture and cell line generation

Sf9 insect cells (Expression Systems) were cultured at 27 °C in suspension in ESF921 media (Expression Systems). For baculovirus generation and passaging, this media was supplemented with 2% fetal bovine serum (FBS), while the media used to grow cells for protein production was not supplemented. HEK293T mammalian cells were cultured at 37 °C and 5% CO_2 in Dulbecco's Modified Eagle Medium (DMEM, Gibco) supplemented with 10% Fetal Bovine Serum (FBS, Gibco), 100 units/mL penicillin (Gibco), and 100 μg/mL streptomycin (Gibco). Tau seeding biosensor cell lines were generated by transducing with lentivirus generated from plasmid pMK1253 [48]. CHIP rescue in CRISPR KO lines was achieved by transducing with lentivirus expressing CHIP variants under control of the constitutive EF1a promoter and co-expression of nuclear-localized blue fluorescent protein (BFP).

Generation of CHIP knockout HEK293T cells

HEK293T cells were edited by transfecting Cas9/sgRNA ribonucleoprotein (RNP) complexes into cells. The guide design and RNP formation were done according to manufacturer specifications (Synthego). Cells were seeded one day prior to transfection, and RNP complexes were transfected using Lipofectamine™ CRISPRMAX™ Cas9 Transfection

Reagent (Thermo Fisher). At 48 hours post-transfection, cells were passaged for subcloning via limited dilution. Knockouts in the resulting monoclonal cell lines were validated by Western blot and ICE analysis of Sanger sequencing results (Synthego).

Recombinant protein expression and purification

Tau constructs were individually subcloned into a 438B pFastBac vector containing an engineered 6xHis tag and a TEV protease cleavage site (Addgene). After confirming their sequence, the vectors were transfected into Sf9 cells to generate baculoviruses. Following two rounds of virus amplification, the proteins were expressed in Sf9 cells by infecting with recombinant baculovirus at 20–40 μL virus per million cells in cell culture flasks and incubated for 3 days at 27 °C with shaking at 120 rpm. Cells are then collected by spinning at 1500 rpm for 20 minutes at 4 °C and stored at −80 °C. The cells are resuspended in Ni lysis buffer (20 mM Tris, pH 8.0, 500 mM KCl, 10 mM imidazole, 10% glycerol) supplemented with EDTA-free protease inhibitor cocktail (Roche) and 6 mM beta-mercaptoethanol. Then, a dounce homogenizer was used to lyse the cells, and the lysates were boiled for 20 mins to denature and precipitate nearly all proteins except for tau. The lysed cells were centrifuged (40000 rpm) at 4 °C for 30 min to clarify and the supernatant was incubated with HisPur Ni-NTA resin (Thermo Scientific) at 4 °C for 1 hour. The resins were then washed and eluted with an elution buffer (20 mM Tris pH 8.0, 100 mM KCl, 6 mM β-mercaptoethanol, and 300 mM imidazole). The fractions containing tau, as judged by SDS-PAGE, were dialyzed with a dialysis buffer (50 mM Tris-HCl, pH 8.0, 100 mM KCl, 6 mM β-mercaptoethanol, 5% glycerol) containing TEV protease to cleave the His tag at 4 °C overnight. The dialyzed proteins were concentrated and applied to a size exclusion column (HiLoad Superdex-200 16/600 column, GE Healthcare) and eluted with PBS buffer (pH 7.4; 1 mM DTT). The concentration of tau was determined by BCA assay (Thermo Scientific) using bovine serum albumin (BSA) as the protein standard. Phosphorylation was confirmed by Western blotting with tau phospho-specific antibodies for tau pS422 (Invitrogen, 1:2000), pS416 (Cell Signaling Technology, 1:2000), pS396 (Thermo Fisher, 1:2000), pT231 (Santa Cruz Biotechnology, 1:2000).

Unmodified tau proteins were expressed in *E.coli* as previously described [19]. Methods for purifying individual TPR proteins are referenced below:

Construct	Vector	Reference for protein purification
0N4R tau WT and variants (insect)	438B	This paper
0N4R tau WT and variants (E.coli)	pMCSG7	This paper
CHIP WT	pET151	[26]
CHIP-K30A	pMCSG7	[26]
PP5	pMCSG7	[35, 48]
HOP	pET151	[35]
DNAJC7	pMCSG7	[35]

Mapping of tau PTMs by liquid chromatography with tandem mass spectrometry

A sample of protein (8 μg) was denatured and reduced with 8 M urea in 100 mM ammonium bicarbonate (pH 8) buffer and 100 mM dithiothreitol (DTT) at 60 °C for 30 minutes, followed by alkylation with 100 mM iodoacetamide at room temperature in the dark for 1 hour. The sample was then incubated 4 hours with trypsin (1:20 weight/weight) at 37 °C. The peptides formed from the digestion were further purified by C18 ZipTips (Millipore) and analyzed by online LC-MS/MS. The MS/MS analyses were conducted using either an Q Exactive Plus Orbitrap (QE) or a Fusion Lumos Orbitrap (Lumos) mass spectrometer (Thermo Scientific). Higher-energy collisional dissociation was used to produce fragmented peptides. The mass resolution of precursor ions was 70000 on the QE and 120000 on the Lumos. The mass resolution of fragment ions was 17500 on the QE and 30000 on the Lumos, respectively. The LC separation was carried out on a NanoAcquity UPLC system (Waters) for both the QE and the Lumos. The LC linear gradient on the QE was increased from 2 – 25% B (0.1% formic acid in acetonitrile) over 48 mins followed by 25 – 37% B over 6 mins and then 37 – 40% B over 3 mins at a flow rate of 400 nL/min. The LC linear gradient on the Lumos was increased from 2 – 5% B over 3 mins followed by 5 – 30% B over 72 mins and then 30 – 50% B over 2 mins at a flow rate of 300 nL/min. The acquired MS/MS raw data was converted into peak lists using an in-house software PAVA and then analyzed using Protein Prospector search engine. The Max. missed cleavages was set to 2. The precursor / fragment mass tolerances were set at 20 ppm / 20 ppm for the QE and 10 ppm / 20 ppm for the Lumos. For all peptides, phosphorylation modification at serine, threonine, and tyrosine residues was selected. Visualization of tau PTMs was performed using Protter [49].

In vitro tau aggregation

Thioflavin T (ThT) assays in 384-well plate (Corning) were performed to measure tau aggregation, as previously described [19]. Briefly, tau (10 μM) samples were incubated with TPR proteins in PBS pH 7.4, 2 mM $MgCl_2$ and 1 mM DTT for 30 min. Then, thioflavin T (Sigma; final concentration 10 μM) was added and aggregation was induced by the addition of a freshly prepared heparin sodium salt solution (MW: 8000 ~ 25000 Da, Santa Cruz) at a final concentration of 100 μg/mL. In competition assays, CHIPOpt peptide was added at the beginning of the reaction. The reactions were carried out at 37 °C with continuous shaking and monitored via fluorescence (excitation=444 nm, emission=485 nm, cutoff=480 nm) in a Spectramax M5 microplate reader (Molecular Devices). Readings were taken every 5 min for a minimum of 24 h. Baseline readings using ThT in tau buffer alone were taken for background subtraction. Baseline-subtracted aggregation curves were then fit to the Gompertz function to calculate lag times. For some curves, fitting required collection of data at timepoints longer than 18 hrs to identify the plateau.

Transmission electron microscopy (TEM)

Electron microscopy of negatively stained Tau aggregates is performed using 600-mesh carbon-coated copper grids (SPI). The samples were incubated for 30 seconds on a glow-discharged grid, and then the solution was removed by filter paper. Three washing steps with double distilled H_2O were followed by three staining steps with 0.75% (w/v) uranyl formate

(Electron Microscopy Sciences). The samples were imaged using a Talos L120C operated at 100 keV. Micrograph images were recorded using a 4kx 4k Thermofisher Scientific Ceta CMOS Camera.

CHIP.tau binding ELISA

CHIP (1 μM) or buffer-matched control was immobilized in 96-well plates (Fisher Scientific, non-sterile, clear, flat-bottom) in CHIP buffer (50 mM HEPES, 10 mM NaCl, pH = 7.4) overnight at 37 °C. The protein was removed, and wells were washed 3X with phosphate-buffered saline with 0.05% Tween-20 (PBS-T) for 3 minutes with rotation at room temperature (RT). Tau samples were prepared as a 3-fold dilution series in tau binding buffer (25 mM HEPES, 40 mM KCl, 8 mM MgCl2, 100 mM NaCl, 0.01% Tween, 1 mM DTT, pH 7.4) and incubated at RT for 3 hours with rotation. Tau was removed, and wells were washed as described. Samples were blocked in 5 % non-fat dry milk in tris-buffered saline (TBS), and then incubated with primary anti-tau (Santa Cruz Biotech, 1:2000) followed by HRP-conjugated secondary antibody (Anaspec, 1:2000). Antibodies were dissolved in 1X TBS with 0.05% Tween-20. Incubations were performed for 1 hour at RT with rotation, separated by wash steps as described. TMB substrate (Thermo Fisher) was then added to the wells and incubated for 15 min at RT, followed by quenching with 1 M HCl. Absorbance readings were performed on a SpectraMax M5 plate reader at OD_{450}. The data was background subtracted to buffer only controls, normalized to maximal binding, and binding curves were fit using non-linear regression in Prism 9.0 (GraphPad).

In vitro ubiquitination assays

4X stock solutions were prepared containing (1) 400 nM Ube1 and 4 μM UbcH5a (R&D Biosystems), (2) 1 mM Ubiquitin (R&D Biosystems), (3) 4 μM CHIP and 4 μM tau substrate and (4) 10 mM ATP and 10 mM $MgCl_2$ (Sigma-Aldrich) in ubiquitination assay buffer (50 mM Tris 50 mM KCl, pH 8.0). Ubiquitination reactions were generated by sequentially adding 10 μL of each 4X stock, ending with ATP/$MgCl_2$, for a final volume of 40 μL (100 nM Ube1, 1 μM UbcH5b, 250 μM ubiquitin, 2.5 mM ATP, 2.5 mM $MgCl_2$, 1 μM CHIP and 1 μM tau substrate). Reactions were incubated at room temperature, and 10 μL aliquots were collected at each time point and quenched in SDS–PAGE loading buffer. Samples were heated to 95 °C, separated by SDS-PAGE, and analyzed by Western blotting with anti-tau (Santa Cruz Biotech, 1:2000) or anti-CHIP antibodies (Abcam, 1:2000). For CHIPopt experiments, CHIPopt was added as a 4X stock along with CHIP and tau substrate and equilibrated for 10 minutes at RT prior to reaction initiation.

Tau cellular seeding assays

HEK293T biosensor cells were seeded at a density of 3500 cells/well in 384-well culture plates (Corning, sterile, black, flat-bottom) in 10%FBS-DMEM containing 0.1 μg/mL Hoechst 33342 (Thermo Fisher Scientific). These cells stably express tauRD, a truncated from of human MAPT composed of four microtubule-binding domains (aa244–368), and including the P301L and V337M mutations, which is fused to mClover [31, 32]. Cells were allowed to adhere for 20 minutes at RT, followed by 3 hours at 37 °C. Aggregated tau samples were diluted in PBS, complexed with Lipofectamine 2000 (Thermo Fisher Scientific) at a tau:Lipofectamine 2000 ratio of 1:16, and incubated for 90 minutes prior to

addition to cells. Following incubation at 37 °C for 72 hours, images for DAPI and FITC channels were acquired from five regions per well using an InCell 6000 (GE Healthcare) high-content microscope and analyzed with InCell Developer software (GE Healthcare) using an algorithm developed to identify aggregates of a minimum size of 0.89 μM^2.

Peptide synthesis

Peptides were synthesized by GenScript to 95% purity by high-performance liquid chromatography. Fluorescence polarization tracer was designed bearing a 5-carboxyfluorescein (5-FAM) fluorophore linked to the N terminus by a six-carbon spacer (aminohexanoic acid). Unlabeled peptides were N-terminally acetylated to enhance stability and solubility. Peptides corresponding to internal tau epitopes were capped with C-terminal amidation, while peptides corresponding to C-terminal epitopes maintained a free C-terminal carboxylate moiety. Peptides were stored as 10 mM stock solutions at −30 °C.

CHIPscore calculations

CHIPScore assigns a value for each amino acid and additionally weights the relative contribution of each residue based on its position within a 5-amino acid peptide [26]. The overall score for each peptide is then linearly summed to achieve its CHIPscore. Here, we determined a CHIPscore for every 5-mer sequence in p.tau ending at a phosphoserine or phosphothreonine, which we reasoned would theoretically serve as putative mimics to the C-terminal aspartate required for binding to CHIP. The affinity for the known partner, Hsp90 (MEEVD, CHIPscore = 1.79), was used as a cutoff.

Competition fluorescence polarization

Fluorescence polarization (FP) assays were run in Corning black 384-well round bottom low volume plate and read on a SpectraMax M5 multimode plate reader at 22°C with a final assay volume of 18 μL. A 2X stock of CHIP + tracer was made in CHIP FP assay buffer (25 mM HEPES, 50 mM KCl, 0.01% Triton X-100, pH 7.4) for a final assay concentration of 1.5 μM CHIP and 20 nM tracer. For protein competition assays, 2X tau protein samples were diluted into CHIP FP buffer, added to CHIP + tracer in a 3-fold dilution series in quadruplicate, and incubated in the dark for 30 minutes at RT prior to reading.

For peptide competition assays, peptide competitor stocks were prepared in CHIP FP dilution buffer (25 mM HEPES pH 7.4, 50 mM KCl 0.01% Triton X-100, 2% DMSO) in three-fold dilutions. 2X CHIP + tracer and peptide competitor solutions were mixed at equal volumes and incubated at RT in the dark for 30 minutes prior to reading. Raw polarization (mP) values were background subtracted to tracer alone and plotted relative to $\log_{10}$ (competitor). Data was fit to the model for [inhibitor] versus response (three parameters) in Prism 9.0 (GraphPad).

Differential scanning fluorimetry

Differential scanning fluorimetry (DSF) was performed in 384-well Axygen quantitative PCR plates (Fisher Scientific) on a qTower real-time PCR thermal cycler (Analytik Jena). Fluorescence intensity readings were taken over 70 cycles in “up-down” mode, where reactions were heated to desired temperature and then cooled to 25 °C before reading.

The temperature was increased 1 °C per cycle. Each well contained 5 μM CHIP, 5X Sypro Orange dye (Thermo Fisher), and 100 μM of peptide in CHIP DSF buffer (25 mM HEPES, 50 mM KCl, 1 mM TCEP, 0.01% CHAPS, 1% DMSO) in a final volume of 15 μL. Fluorescence intensity data were truncated between 30 and 60 °C, plotted relative to temperature, and fit to a Boltzmann Sigmoid in Prism 9.0 (GraphPad).

TauRD co-immunoprecipitation

HEK293T biosensor cells were lysed in immunoprecipitation (IP) lysis buffer (25 mM Tris-HCl, 150 mM NaCl, 1 mM EDTA, 1% NP-40, 5% glycerol, pH 7.4) on ice for 15 minutes with periodic agitation. Lysates were separated by centrifugation at 13000 RPM for 10 minutes at 4 °C, and supernatants were collected. A representative input sample was collected, and SDS-PAGE loading buffer was added to 1X. Lysates were diluted to 1000 μL, and washed Chromotek magnetic GFP-trap agarose beads (Proteintech) were added. Samples were incubated for 1 hour at 4 °C with rotation. Following, beads were collected on a magnet, and the supernatants were discarded. Beads were washed 3X in ice-cold IP lysis buffer, and immunoprecipitated complexes were eluted by incubation with 2X SDS-PAGE loading buffer at 95 °C for 5 minutes. Inputs and eluted samples were separated by SDS-PAGE using stain-free gels (BioRad) and analyzed by Western blotting with antibodies for the tauRD (Cell Signaling Technology, 1:2000), CHIP (Abcam, 1:2000), or Hsp70 (Santa Cruz Biotechnology, 1:2000). Stain-free visualization was used as a loading control.

Supplementary Material

Refer to Web version on PubMed Central for supplementary material.

ACKNOWLEDGEMENTS

This manuscript is dedicated to Peter Wright's contributions to the field. The work was supported by grants from the Alzheimer's Association (CMD, KL), National Institutes of Health AG068125 (JEG, DRS, CSC) and F31AG077842 (MC) and the Tau Consortium (JEG, DRS). We acknowledge Darren Hutt (UCSF) for assistance with the seeding assays, Kathy Li and Al Burlingame (UCSF) for assistance with the mass spectrometry and Eric Tse (UCSF) for maintenance of the electron microscopes.

ABBREVIATIONS

AD	Alzheimer's disease
CHIP	C-terminus of Hsp70-interacting protein
FTD	frontotemporal dementia
HOP	Hsp70/Hsp90 organizing protein
Hsc70	heat shock cognate protein 70 KDa
MAPT/tau	Microtubule-associated protein tau
tauRD	tau repeat domain
TPR	tetratricopeptide repeat

PP5	protein phosphatase 5

REFERENCES

[1]. Spires-Jones TL, Stoothoff WH, de Calignon A, Jones PB, Hyman BT. Tau pathophysiology in neurodegeneration: a tangled issue. Trends Neurosci. 2009;32:150–9. [PubMed: 19162340]

[2]. Cabrales Fontela Y, Kadavath H, Biernat J, Riedel D, Mandelkow E, Zweckstetter M. Multivalent cross-linking of actin filaments and microtubules through the microtubule-associated protein Tau. Nature communications. 2017;8:1981.

[3]. Wang Y, Mandelkow E. Tau in physiology and pathology. Nat Rev Neurosci. 2016;17:5–21. [PubMed: 26631930]

[4]. Kadavath H, Hofele RV, Biernat J, Kumar S, Tepper K, Urlaub H, et al. Tau stabilizes microtubules by binding at the interface between tubulin heterodimers. Proc Natl Acad Sci U S A. 2015;112:7501–6. [PubMed: 26034266]

[5]. Bramblett GT, Goedert M, Jakes R, Merrick SE, Trojanowski JQ, Lee VM. Abnormal tau phosphorylation at Ser396 in Alzheimer's disease recapitulates development and contributes to reduced microtubule binding. Neuron. 1993;10:1089–99. [PubMed: 8318230]

[6]. Despres C, Byrne C, Qi H, Cantrelle FX, Huvent I, Chambraud B, et al. Identification of the Tau phosphorylation pattern that drives its aggregation. Proc Natl Acad Sci U S A. 2017;114:9080–5. [PubMed: 28784767]

[7]. Haj-Yahya M, Gopinath P, Rajasekhar K, Mirbaha H, Diamond MI, Lashuel HA. Site-Specific Hyperphosphorylation Inhibits, Rather than Promotes, Tau Fibrillization, Seeding Capacity, and Its Microtubule Binding. Angew Chem Int Ed Engl. 2020;59:4059–67. [PubMed: 31863676]

[8]. Plouffe V, Mohamed NV, Rivest-McGraw J, Bertrand J, Lauzon M, Leclerc N. Hyperphosphorylation and cleavage at D421 enhance tau secretion. PLoS One. 2012;7:e36873. [PubMed: 22615831]

[9]. Mair W, Muntel J, Tepper K, Tang S, Biernat J, Seeley WW, et al. FLEXITau: Quantifying Post-translational Modifications of Tau Protein in Vitro and in Human Disease. Anal Chem. 2016;88:3704–14. [PubMed: 26877193]

[10]. Barthelemy NR, Li Y, Joseph-Mathurin N, Gordon BA, Hassenstab J, Benzinger TLS, et al. A soluble phosphorylated tau signature links tau, amyloid and the evolution of stages of dominantly inherited Alzheimer's disease. Nat Med. 2020;26:398–407. [PubMed: 32161412]

[11]. Wesseling H, Mair W, Kumar M, Schlaffner CN, Tang S, Beerepoot P, et al. Tau PTM Profiles Identify Patient Heterogeneity and Stages of Alzheimer's Disease. Cell. 2020;183:1699–713 e13. [PubMed: 33188775]

[12]. Augustinack JC, Schneider A, Mandelkow EM, Hyman BT. Specific tau phosphorylation sites correlate with severity of neuronal cytopathology in Alzheimer's disease. Acta Neuropathol. 2002;103:26–35. [PubMed: 11837744]

[13]. Jinwal UK, O'Leary JC 3rd, Borysov SI, Jones JR, Li Q, Koren J 3rd, et al. Hsc70 rapidly engages tau after microtubule destabilization. J Biol Chem. 2010;285:16798–805. [PubMed: 20308058]

[14]. Fontaine SN, Martin MD, Akoury E, Assimon VA, Borysov S, Nordhues BA, et al. The active Hsc70/tau complex can be exploited to enhance tau turnover without damaging microtubule dynamics. Hum Mol Genet. 2015;24:3971–81. [PubMed: 25882706]

[15]. Fontaine SN, Rauch JN, Nordhues BA, Assimon VA, Stothert AR, Jinwal UK, et al. Isoform-selective Genetic Inhibition of Constitutive Cytosolic Hsp70 Activity Promotes Client Tau Degradation Using an Altered Co-chaperone Complement. J Biol Chem. 2015;290:13115–27. [PubMed: 25864199]

[16]. Jinwal UK, Miyata Y, Koren J 3rd, Jones JR, Trotter JH, Chang L, et al. Chemical manipulation of hsp70 ATPase activity regulates tau stability. J Neurosci. 2009;29:12079–88. [PubMed: 19793966]

[17]. Young ZT, Rauch JN, Assimon VA, Jinwal UK, Ahn M, Li X, et al. Stabilizing the Hsp70-Tau Complex Promotes Turnover in Models of Tauopathy. Cell chemical biology. 2016;23:992–1001. [PubMed: 27499529]

[18]. Freilich R, Arhar T, Abrams JL, Gestwicki JE. Protein-Protein Interactions in the Molecular Chaperone Network. Acc Chem Res. 2018;51:940–9. [PubMed: 29613769]

[19]. Mok SA, Condello C, Freilich R, Gillies A, Arhar T, Oroz J, et al. Mapping interactions with the chaperone network reveals factors that protect against tau aggregation. Nat Struct Mol Biol. 2018;25:384–93. [PubMed: 29728653]

[20]. Yuste-Checa P, Trinkaus VA, Riera-Tur I, Imamoglu R, Schaller TF, Wang H, et al. The extracellular chaperone Clusterin enhances Tau aggregate seeding in a cellular model. Nature communications. 2021;12:4863.

[21]. Baughman HER, Pham TT, Adams CS, Nath A, Klevit RE. Release of a disordered domain enhances HspB1 chaperone activity toward tau. Proc Natl Acad Sci U S A. 2020;117:2923–9. [PubMed: 31974309]

[22]. Hou Z, Wydorski PM, Perez VA, Mendoza-Oliva A, Ryder BD, Mirbaha H, et al. DnaJC7 binds natively folded structural elements in tau to inhibit amyloid formation. Nature communications. 2021;12:5338.

[23]. Zhang S, Zhu Y, Lu J, Liu Z, Lobato AG, Zeng W, et al. Specific binding of Hsp27 and phosphorylated Tau mitigates abnormal Tau aggregation-induced pathology. eLife. 2022;11.

[24]. Giustiniani J, Guillemeau K, Dounane O, Sardin E, Huvent I, Schmitt A, et al. The FK506-binding protein FKBP52 in vitro induces aggregation of truncated Tau forms with prion-like behavior. FASEB J. 2015;29:3171–81. [PubMed: 25888602]

[25]. Blair LJ, Nordhues BA, Hill SE, Scaglione KM, O'Leary JC 3rd, Fontaine SN, et al. Accelerated neurodegeneration through chaperone-mediated oligomerization of tau. J Clin Invest. 2013;123:4158–69. [PubMed: 23999428]

[26]. Ravalin M, Theofilas P, Basu K, Opoku-Nsiah KA, Assimon VA, Medina-Cleghorn D, et al. Specificity for latent C termini links the E3 ubiquitin ligase CHIP to caspases. Nat Chem Biol. 2019;15:786–94. [PubMed: 31320752]

[27]. Gong CX, Liu F, Wu G, Rossie S, Wegiel J, Li L, et al. Dephosphorylation of microtubule-associated protein tau by protein phosphatase 5. J Neurochem. 2004;88:298–310. [PubMed: 14690518]

[28]. Moll A, Ramirez LM, Ninov M, Schwarz J, Urlaub H, Zweckstetter M. Hsp multichaperone complex buffers pathologically modified Tau. Nature communications. 2022;13:3668.

[29]. Tepper K, Biernat J, Kumar S, Wegmann S, Timm T, Hubschmann S, et al. Oligomer formation of tau protein hyperphosphorylated in cells. J Biol Chem. 2014;289:34389–407. [PubMed: 25339173]

[30]. Zhang W, Falcon B, Murzin AG, Fan J, Crowther RA, Goedert M, et al. Heparin-induced tau filaments are polymorphic and differ from those in Alzheimer's and Pick's diseases. eLife. 2019;8.

[31]. Kfoury N, Holmes BB, Jiang H, Holtzman DM, Diamond MI. Trans-cellular propagation of Tau aggregation by fibrillar species. J Biol Chem. 2012;287:19440–51. [PubMed: 22461630]

[32]. Chen JJ, Nathaniel DL, Raghavan P, Nelson M, Tian R, Tse E, et al. Compromised function of the ESCRT pathway promotes endolysosomal escape of tau seeds and propagation of tau aggregation. J Biol Chem. 2019;294:18952–66. [PubMed: 31578281]

[33]. Strang KH, Golde TE, Giasson BI. MAPT mutations, tauopathy, and mechanisms of neurodegeneration. Lab Invest. 2019;99:912–28. [PubMed: 30742061]

[34]. Yoshiyama Y, Higuchi M, Zhang B, Huang SM, Iwata N, Saido TC, et al. Synapse loss and microglial activation precede tangles in a P301S tauopathy mouse model. Neuron. 2007;53:337–51. [PubMed: 17270732]

[35]. Assimon VA, Southworth DR, Gestwicki JE. Specific Binding of Tetratricopeptide Repeat Proteins to Heat Shock Protein 70 (Hsp70) and Heat Shock Protein 90 (Hsp90) Is Regulated by Affinity and Phosphorylation. Biochemistry. 2015;54:7120–31. [PubMed: 26565746]

[36]. Munari F, Mollica L, Valente C, Parolini F, Kachoie EA, Arrigoni G, et al. Structural Basis for Chaperone-Independent Ubiquitination of Tau Protein by Its E3 Ligase CHIP. Angew Chem Int Ed Engl. 2022;61:e202112374.

[37]. Dickey CA, Yue M, Lin WL, Dickson DW, Dunmore JH, Lee WC, et al. Deletion of the ubiquitin ligase CHIP leads to the accumulation, but not the aggregation, of both endogenous phospho- and caspase-3-cleaved tau species. J Neurosci. 2006;26:6985–96. [PubMed: 16807328]

[38]. Shimura H, Schwartz D, Gygi SP, Kosik KS. CHIP-Hsc70 complex ubiquitinates phosphorylated tau and enhances cell survival. J Biol Chem. 2004;279:4869–76. [PubMed: 14612456]

[39]. Petrucelli L, Dickson D, Kehoe K, Taylor J, Snyder H, Grover A, et al. CHIP and Hsp70 regulate tau ubiquitination, degradation and aggregation. Hum Mol Genet. 2004;13:703–14. [PubMed: 14962978]

[40]. Zhang YJ, Xu YF, Liu XH, Li D, Yin J, Liu YH, et al. Carboxyl terminus of heat-shock cognate 70-interacting protein degrades tau regardless its phosphorylation status without affecting the spatial memory of the rats. J Neural Transm (Vienna). 2008;115:483–91. [PubMed: 18301957]

[41]. Sahara N, Murayama M, Mizoroki T, Urushitani M, Imai Y, Takahashi R, et al. In vivo evidence of CHIP up-regulation attenuating tau aggregation. J Neurochem. 2005;94:1254–63. [PubMed: 16111477]

[42]. Nicholls SB, DeVos SL, Commins C, Nobuhara C, Bennett RE, Corjuc DL, et al. Characterization of TauC3 antibody and demonstration of its potential to block tau propagation. PLoS One. 2017;12:e0177914.

[43]. Wang Y, Guan S, Acharya P, Liu Y, Thirumaran RK, Brandman R, et al. Multisite phosphorylation of human liver cytochrome P450 3A4 enhances Its gp78- and CHIP-mediated ubiquitination: a pivotal role of its Ser-478 residue in the gp78-catalyzed reaction. Mol Cell Proteomics. 2012;11:M111 010132.

[44]. Wang Y, Kim SM, Trnka MJ, Liu Y, Burlingame AL, Correia MA. Human liver cytochrome P450 3A4 ubiquitination: molecular recognition by UBC7-gp78 autocrine motility factor receptor and UbcH5a-CHIP-Hsc70-Hsp40 E2–E3 ubiquitin ligase complexes. J Biol Chem. 2015;290:3308–32. [PubMed: 25451919]

[45]. Powers ET, Morimoto RI, Dillin A, Kelly JW, Balch WE. Biological and chemical approaches to diseases of proteostasis deficiency. Annu Rev Biochem. 2009;78:959–91. [PubMed: 19298183]

[46]. Lamande SR, Bateman JF. Procollagen folding and assembly: the role of endoplasmic reticulum enzymes and molecular chaperones. Semin Cell Dev Biol. 1999;10:455–64. [PubMed: 10597628]

[47]. Smith LM, Kelleher NL, Consortium for Top Down P. Proteoform: a single term describing protein complexity. Nat Methods. 2013;10:186–7. [PubMed: 23443629]

[48]. Connarn JN, Assimon VA, Reed RA, Tse E, Southworth DR, Zuiderweg ER, et al. The molecular chaperone Hsp70 activates protein phosphatase 5 (PP5) by binding the tetratricopeptide repeat (TPR) domain. J Biol Chem. 2014;289:2908–17. [PubMed: 24327656]

[49]. Omasits U, Ahrens CH, Muller S, Wollscheid B. Protter: interactive protein feature visualization and integration with experimental proteomic data. Bioinformatics. 2014;30:884–6. [PubMed: 24162465]

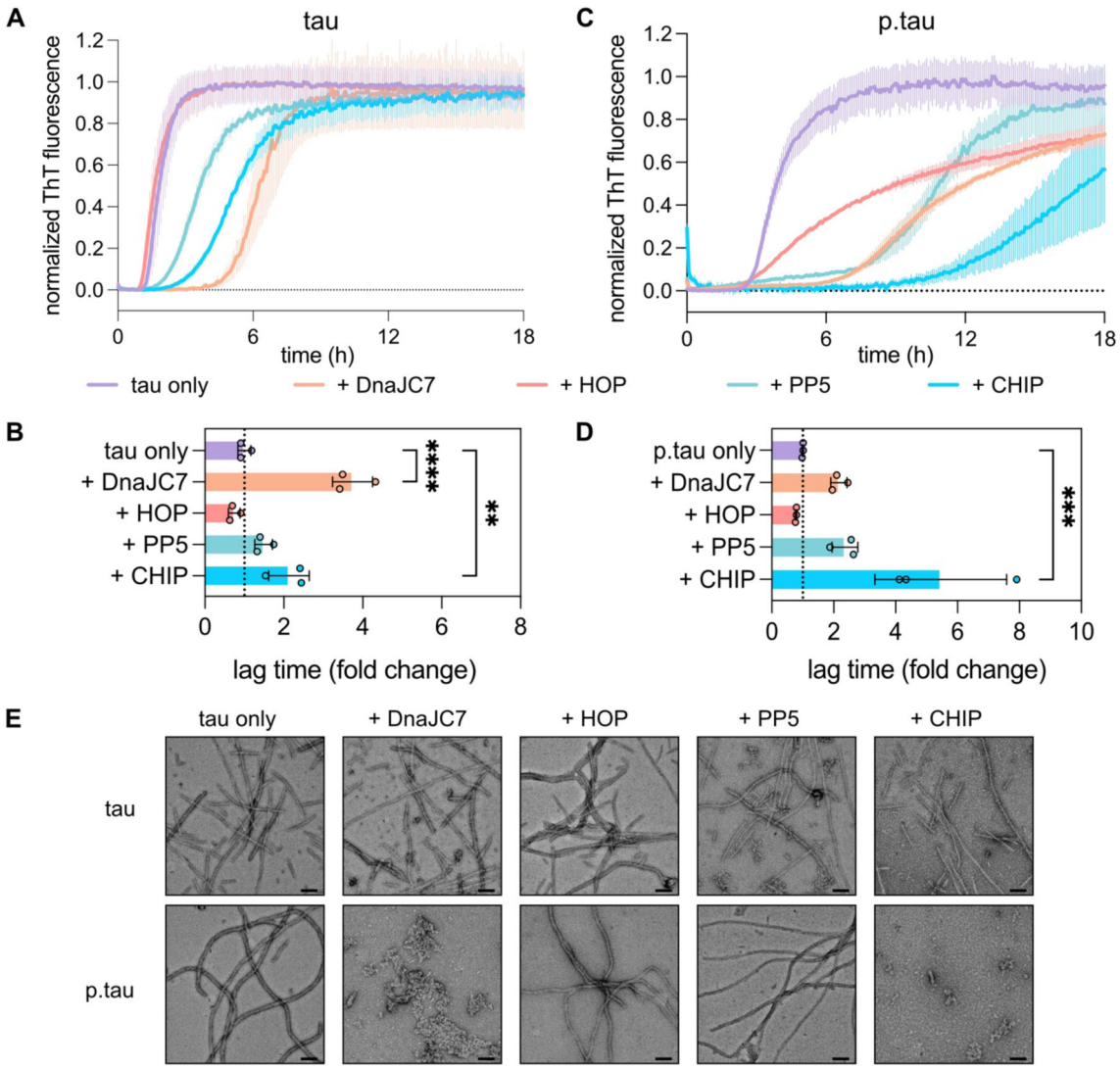

Figure 1: Amongst the TPR chaperones, CHIP preferentially suppresses p.tau aggregation.

(A) ThT curves of unmodified tau aggregation in the presence of TPR cochaperones. Data is shown as mean ± SEM (n=3). Tau concentration is 10 μM and TPR protein concentrations are 10 μM. **(B)** Lag time for unmodified tau aggregation in the presence of TPR cochaperones derived from (A). Data is normalized to tau alone and represented as mean ± SD. Statistical significance was determined by one-way analysis of variance (ANOVA) with Dunnett's post-hoc test (**p<0.01, ****p<0.0001). **(C)** ThT curves of phosphorylated tau (p.tau) aggregation in the presence of TPR cochaperones. Data is shown as mean ± SEM (n=3). Tau concentration is 10 μM and TPR protein concentrations are 10 μM **(D)** Lag time for unmodified tau aggregation in the presence of TPR cochaperones derived from (C). Data is shown relative to tau alone and represented as mean ± SD. Statistical significance was determined by one-way ANOVA with Dunnett's post-hoc test (***p<0.001). **(E)** TEM micrographs of tau or p.tau samples (10 μM) following 24-hour fibrillization in the presence of TPR co-chaperones (10 μM). Scale bar represents 100 nm. Data shown is representative of two replicate experiments.

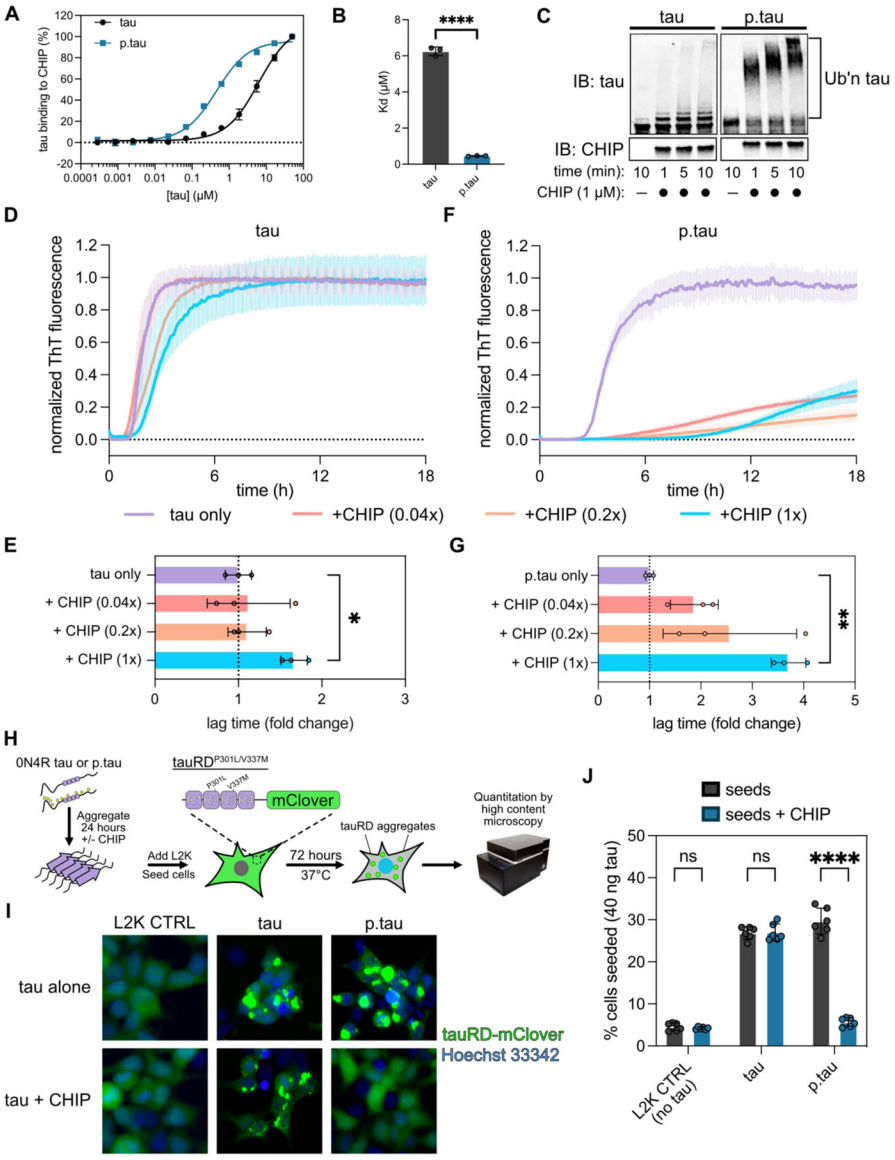

Figure 2: CHIP preferentially inhibits aggregation and seeding of phosphorylated tau.

(A) Affinity comparison of CHIP interaction with unmodified or phosphorylated tau. Increasing concentrations of tau proteoforms were incubated with immobilized CHIP (see Methods) and binding was analyzed by ELISA. Data is shown as mean ± SD (n=3). **(B)** Equilibrium binding constants for CHIP.tau interactions as determined in (A). Data is shown as mean ± SD (n=3). Statistical significance was determined by student's unpaired t-test (****p<0.0001). **(C)** Ubiquitination of tau variants by CHIP *in vitro*. Unmodified or phosphorylated tau (4 μM) was incubated with CHIP (4 μM), ubiquitination machinery, and ATP/$MgCl_2$ for the indicated times and analyzed by immunoblotting. Samples lacking CHIP were used as controls. Ub'n = ubiquitinated. Data shown is representative of two replicate experiments. **(D)** ThT curves for tau (10 μM) aggregation in the presence of varying molar ratios of CHIP. Data is shown as mean ± SEM (n=3). **(E)** Lag time for unmodified tau aggregation in the presence of varying molar ratios of CHIP derived from (D). Data is

shown relative to tau alone and represented as mean ± SD. Statistical significance was determined by one-way ANOVA with Dunnett's post-hoc test (*p<0.05). **(F)** ThT curves for p.tau (10 μM) aggregation in the presence of varying molar ratios of CHIP. Data is shown as mean ± SEM (n=3). **(G)** Lag time for p.tau aggregation in the presence of varying molar ratios of CHIP derived from (F). Data is shown relative to tau alone and represented as mean ± SEM. Statistical significance was determined by one-way ANOVA with Dunnet's post-hoc test (**p<0.01). **(H)** Model for tau seeding assay workflow. Tau seeding samples were prepared by incubating tau or p.tau (10 μM) with CHIP (10 μM) for 24 hrs, as above. **(I)** Representative fluorescence microscopy images showing seeded aggregation of tauRD-mClover in HEK293T biosensor cells after 72-hour incubation. **(J)** Quantitation of tau aggregation in HEK293T biosensor cells after seeding with tau or p.tau fibrils formed in the absence or presence of CHIP. Lipofectamine 2000 (L2K CTRL) without tau was used as a negative control. Data is shown as mean ± SD (n=6). Statistical significance was determined by two-way ANOVA with Bonferroni's post-hoc test (****p<0.0001, ns = p>0.05).

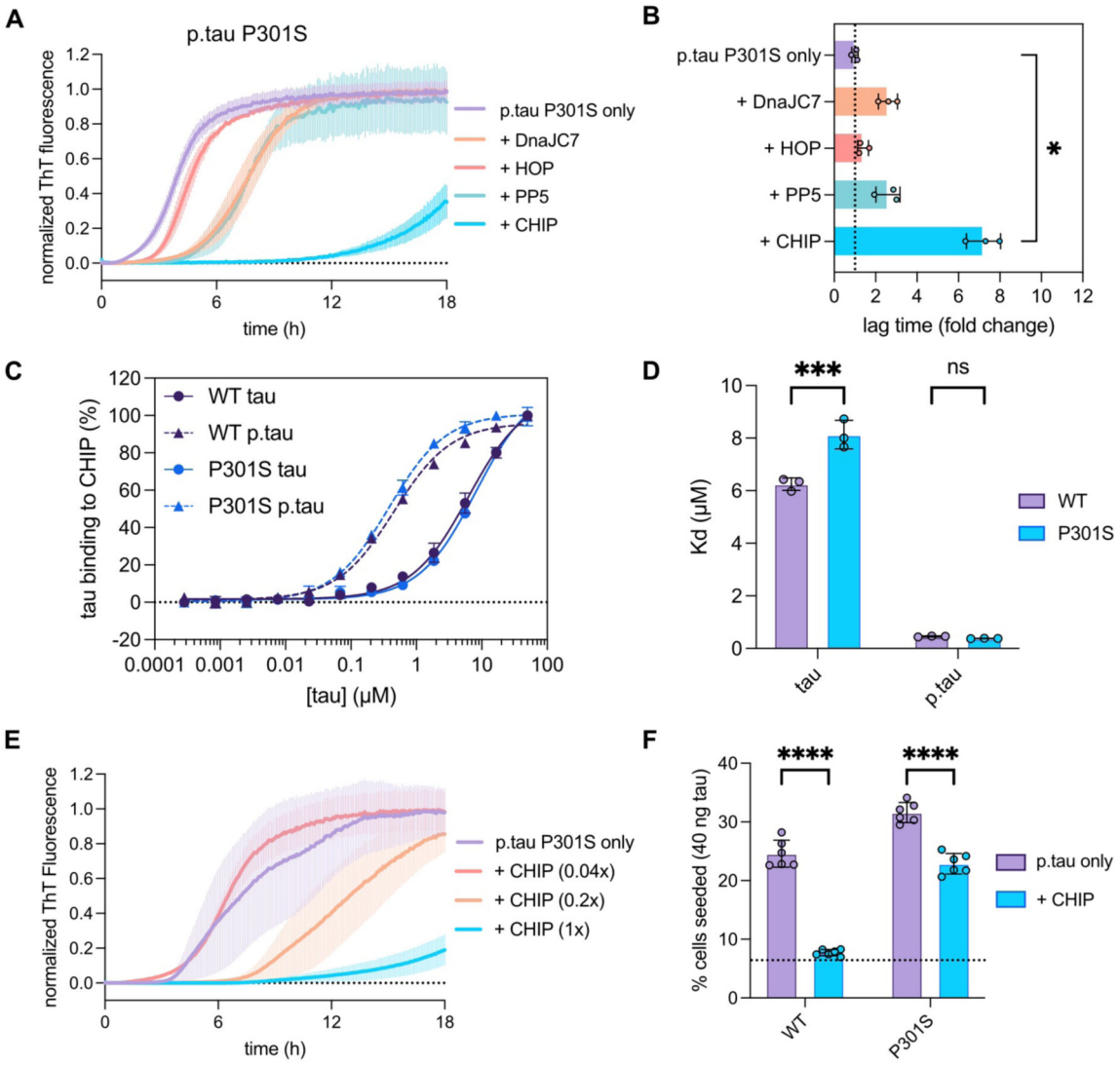

Figure 3: CHIP restricts aggregation and seeding of disease-associated P301S mutant phospho-tau

(A) ThT curves for p.tau P301S aggregation in the presence of various TPR cochaperones. Data is shown as mean ± SEM (n=3). Tau concentration is 10 μM and TPR protein concentrations were 10 μM. **(B)** Lag time for P301S p.tau aggregation in the presence of various cochaperones derived from (A). Data is shown relative to p.tau alone and represented as mean ± SD. Statistical significance was determined by one-way ANOVA with Dunnett's post-hoc test (*$p<0.05$). **(C)** Affinity comparison of CHIP interaction with WT (purple) or P301S (blue) unmodified (solid) tau or p.tau (dashed). Increasing concentrations of tau proteoforms were incubated with immobilized CHIP and analyzed by ELISA. Data is shown as mean ± SD (n=3). **(D)** Equilibrium binding constants for CHIP.tau interactions as determined in (D). Data is shown as mean ± SD (n=3). Statistical significance was determined by one-way ANOVA with Bonferroni's post-hoc test (***$p<0.001$, ns = $p>0.05$). **(E)** ThT curve of p.tau P301S (10 μM) aggregation in the presence of varying molar ratios of CHIP. Data is shown as mean ± SEM (n=3). **(F)** Quantitation of tau aggregation

in HEK293T biosensor cells after seeding with WT or P301S p.tau fibrils formed in the absence or presence of CHIP. Data is shown as mean ± SEM (n=6). Statistical significance was determined by one-way ANOVA with Bonferroni's post-hoc test (****$p<0.0001$).

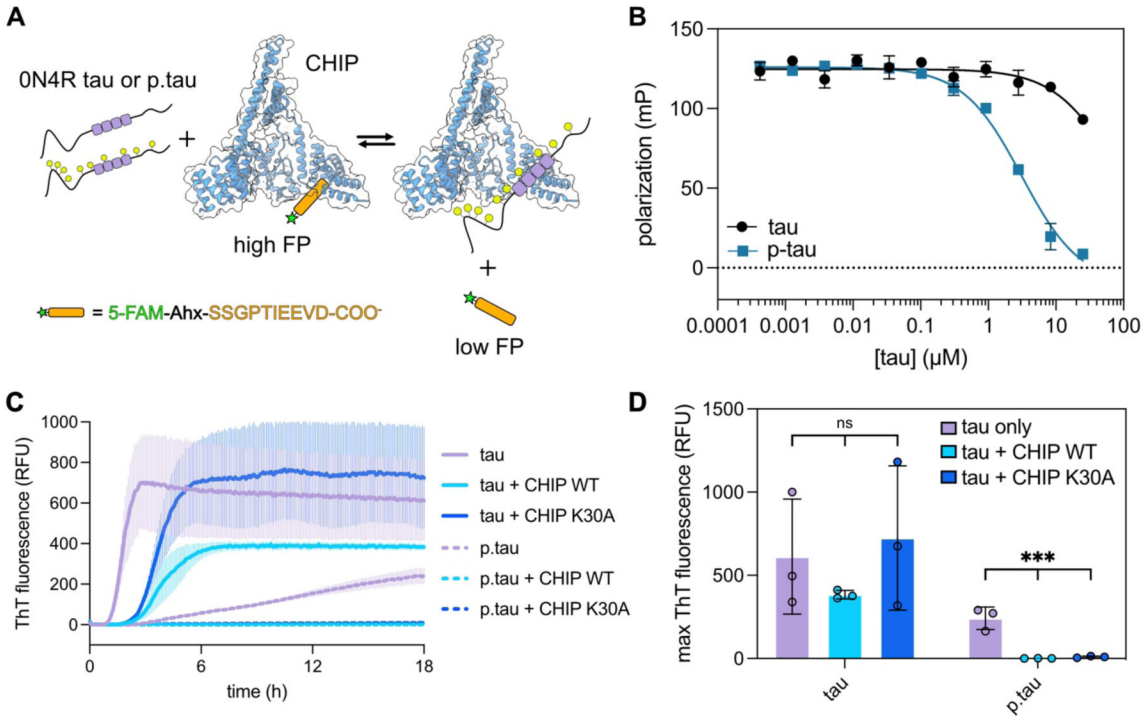

Figure 4: CHIP recognizes p.tau through a distinct TPR binding mode

(A) Workflow of the fluorescence polarization (FP) assay used to measure binding to CHIP's TPR domain. Briefly, CHIP (blue, PDB: 2C2L) is bound to a fluorescent tracer (orange) and displacement by tau or p.tau (purple) leads to a decrease in FP signal (mP). 5-FAM = 5-carboxyfluorescein; Ahx = 6-aminohexanoic acid. **(B)** Competition curves for CHIP-tracer interactions in the presence of tau or p.tau. Data is shown as mean ± SD (n=4). **(C)** ThT curves of tau (solid lines) or p.tau (dashed lines) aggregation in the absence or presence of WT or K30A mutant CHIP. Data is shown as mean ± SEM (n=3). Tau concentration is 10 μM and CHIP WT and CHIP K30A concentrations are 10 μM. **(D)** Max ThT fluorescence after 18 hours of tau aggregation in the presence of WT or mutant CHIP derived from (C). Data is shown as mean ± SD (n=3). Statistical significance was determined compared to tau only by one-way ANOVA with Dunnett's post-hoc test (***$p<0.001$, ns = $p>0.05$).

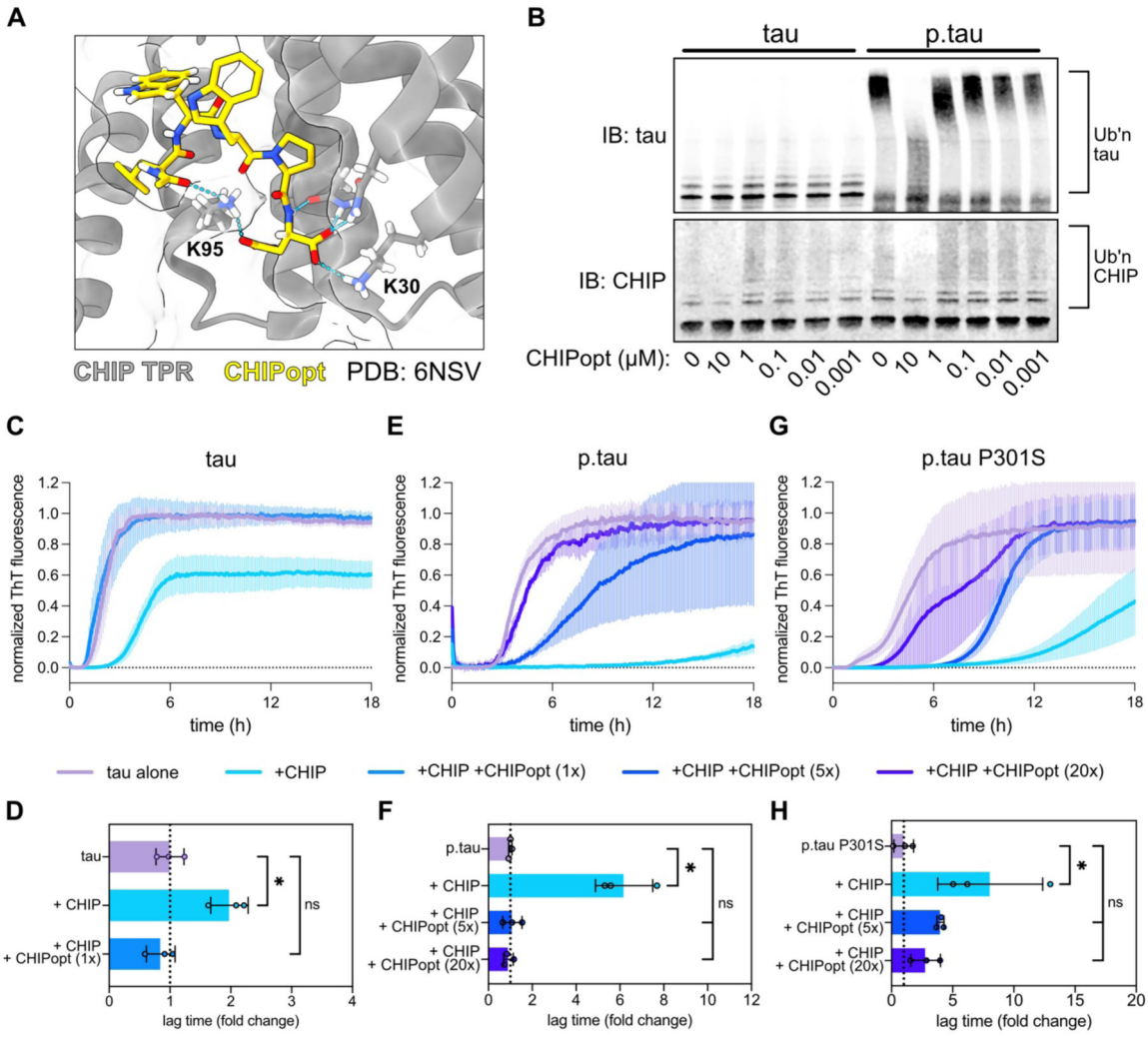

Figure 5: The CHIP TPR domain is required for anti-aggregation activity

(A) Structural depiction of CHIPopt peptide (yellow) binding to CHIP's TPR domain (grey) (PDB 6NSV), highlighting the interactions between the aspartate side chain and C-terminal carboxylate of CHIPopt, which are are coordinated by CHIP's residues K30 and K95. **(B)** Ubiquitination of tau variants (4 μM) by CHIP (4 μM) *in vitro* in the presence of CHIPopt. Tau or p.tau was incubated with CHIP, ubiquitination machinery, ATP/$MgCl_2$, and the indicated concentration of CHIPopt for 10 minutes and analyzed by immunoblotting. Samples lacking CHIPopt were used as controls. Ub'n = ubiquitinated. Data shown is representative of two replicate experiments. **(C)** ThT curves of tau (10 μM) aggregation in the presence of CHIP (10 μM) and the indicated molar ratio of CHIPopt. Data is shown as mean ± SEM (n=3). **(D)** Lag time for of tau aggregation in the presence of CHIP and the indicated molar ratio of CHIPopt derived from (C). Data is normalized to tau alone and represented as mean ± SD (n=3). Statistical significance was determined by one-way ANOVA with Dunnett's post-hoc test (*$p<0.05$, ns = $p>0.05$). **(E)** ThT curves of p.tau (10 μM) aggregation in the presence of CHIP (10 μM) and the indicated molar ratio of CHIPopt. Data is shown as mean ± SEM (n=3). **(F)** Lag time for of p.tau (10 μM) aggregation in the presence of CHIP (10 μM) and the indicated molar ratio of CHIPopt derived from (E).

Data is shown relative to tau alone and represented as mean ± SD. Statistical significance was determined by one-way ANOVA with Dunnett's post-hoc test (*p<0.05, ns = p>0.05). **(G)** ThT curves of p.tau P301S (10 μM) aggregation in the presence of CHIP (10 μM) and the indicated molar ratio of CHIPopt. Data is shown as mean ± SEM (n=3). **(H)** Lag time for p.tau P301S aggregation in the presence of CHIP and the indicated molar ratio of CHIPopt derived from (G). Data is shown relative to tau alone and represented as mean ± SD. Statistical significance was determined by one-way ANOVA with Dunnett's post-hoc test (*p<0.05, ns = p>0.05).

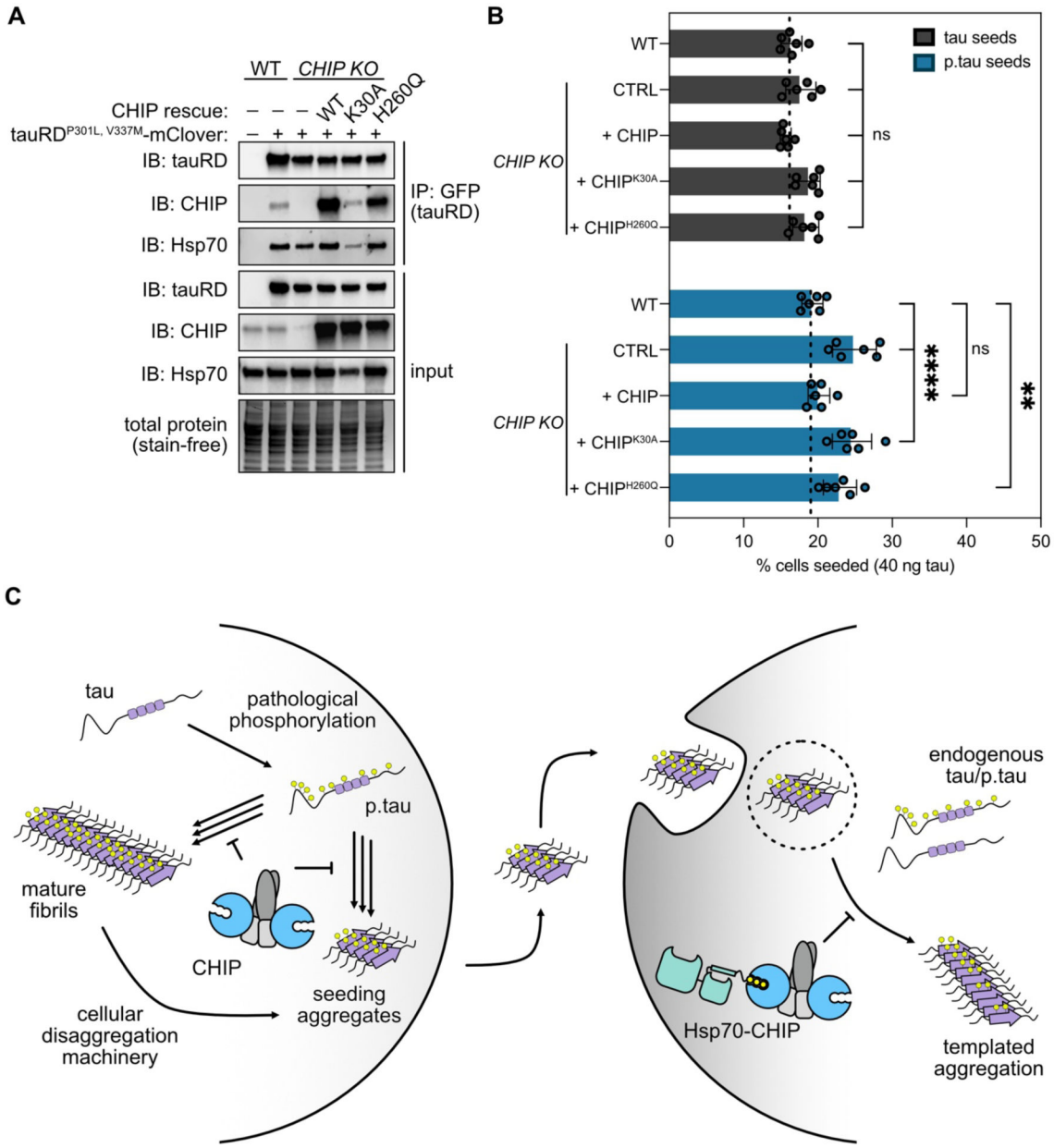

Figure 6: Endogenous CHIP restricts seeded aggregation of phospho-tau

(A) Co-immunoprecipitation (co-IP) of tauRD complexes from HEK293T biosensor cells. TauRD-mClover was immunoprecipitated, and the resulting amount of CHIP and Hsp70 in the sample was analyzed by immunoblotting (see Methods). WT HEK293T cells not expressing the tau biosensor were used as control, and protein loading was confirmed by stain-free gel. Data shown is representative of two replicate experiments. **(B)** Quantitation of tau aggregation in HEK293T biosensor cell lines after seeding with tau or p.tau fibrils. The seeding samples were prepared as above (tau (10 μM), 24 hrs). Data is shown as mean ± SD (n=6). Statistical significance was determined by two-way ANOVA with Bonferroni's post-hoc test (**p<0.01,****p<0.0001, ns = p>0.05). **(C)** Model for CHIP regulation of p.tau aggregation and seeding. Tau is pathologically phosphorylated amidst the progression

of neurodegenerative diseases, which promotes the formation of fibrillar species that seed aggregation in a transcellular manner. In the donor cell (left), CHIP directly interacts with monomeric p.tau to inhibit the formation of mature fibrils or seeding aggregates. In the recipient cell (right), CHIP selectively blocks the templated aggregation of phosphorylated tau by stabilizing a ternary complex of CHIP, p.tau, and Hsp70.